Complete pump depletion by autoresonant second harmonic generation in a nonuniform medium

Oded Yaakobi,[1,*] Matteo Clerici,[1,2] Lucia Caspani,[1] François Vidal,[1] and Roberto Morandotti[1]

[1]*INRS-EMT, University of Québec, 1650 Boul. Lionel-Boulet, Varennes, Québec J3X 1S2 Canada*
[2]*School of Engineering and Physical Sciences, Heriot-Watt University, Edinburgh EH14 4AS, UK*
**Corresponding author: oded.yaakobi@emt.inrs.ca*

In this paper, we develop for the first time to our knowledge an analytical theory of second harmonic generation (SHG) in a generic nonuniform $\chi^{(2)}$ medium. It is shown that by varying the properties of the medium gradually enough, the system can enter an autoresonant state in which the phases of the fundamental pump and of the generated second harmonic wave are locked. The effect of autoresonance allows efficient transfer of energy between the waves and, due to the continuous phase-locking in the system, all the energy of the pump could be converted to the second harmonic. Simple closed-form expressions for the waves amplitudes as a function of the longitudinal coordinate are derived, and an explicit criterion for the stability of the autoresonant state is obtained. Our analytical theory is compared to the numerical solution of the coupled mode equations, which are found to be in excellent agreement with each other. The analytical closed-form expressions that we derive could be very useful for practical design of SHG devices with increased performances, such as highly efficient, wideband frequency converters.

OCIS codes: (190.7220) Upconversion; (190.4223) Nonlinear wave mixing; (190.4410) Nonlinear optics, parametric processes; (190.7070) Two-wave mixing; (190.4975) Parametric processes; (230.7405) Wavelength conversion devices.

1. INTRODUCTION

Second harmonic generation (SHG) is among the simplest processes of nonlinear optics and involves the conversion of energy from a fundamental pump wave at frequency ω_1 to its second harmonic at frequency $\omega_2 = 2\omega_1$ [1]. Since the pioneering studies of nonlinear optics at the beginning of the 1960s [2,3], SHG was studied extensively in various types of materials and configurations and has been exploited in numerous applications. Over the years, various theoretical and experimental studies have shown that in many systems, the SHG conversion efficiency and bandwidth could be increased by varying the properties of the medium along the direction of the waves propagation [4–8]. Similar conclusions were obtained in other parametric processes, e.g., two-step third-harmonic generation [9], three-wave mixing (TWM) in the undepleted pump regime [10–12], and also TWM and four-wave mixing (FWM) where pump-depletion was taken into account [13–15].

In this paper, we develop an analytical theory of SHG in a generic spatially dependent $\chi^{(2)}$ medium and support it by comparison with numerical simulations in plane, monochromatic wave conditions. One of the most significant results of our theory is the derivation of simple, closed-form expressions for the energy distribution between the fundamental and the generated second-harmonic waves along propagation. Moreover, we define the conditions in which the conversion efficiency could be improved, eventually leading to complete pump depletion. It should be emphasized that these conditions differ from the corresponding criteria in a TWM process in nonuniform media (see [14]) and cannot be derived from them as some sort of a specific degenerate case. We show that the dynamics of the considered system could be explained in terms of the autoresonance effect. In autoresonance, a nonlinear wave or oscillator maintains a continuous phase-locking with (an) other wave(s) or with an external driving force due to a gradual variation of the parameters of the system in time or space. Utilizing autoresonance in wave-mixing processes allows to transfer energy between one type of wave or mode in the system to another with very high conversion efficiency. The attractive advantages of autoresonant wave mixing have already been demonstrated in additional processes to those mentioned above, e.g., two-wave interaction in nonlinear optics [16,17] and stimulated Raman scattering in plasmas [18–23].

2. MATHEMATICAL MODEL

We start by writing the envelope equations describing the process of SHG for plane, monochromatic waves in a nonuniform $\chi^{(2)}$ medium where $\omega_2 = 2\omega_1$ [1]:

$$\frac{dA_1}{dz} = i\eta_1 A_1^* A_2 e^{-i\int_0^z \Delta k(z')\mathrm{d}z'}, \tag{1}$$

$$\frac{dA_2}{dz} = i\frac{\eta_2}{2} A_1^2 e^{+i\int_0^z \Delta k(z')\mathrm{d}z'}. \tag{2}$$

The coupling coefficients are defined by $\eta_j = 2d_{\mathrm{eff}}\omega_j^2/(k_j c^2)$ where c is the speed of light in vacuum and d_{eff} is the effective nonlinear susceptibility. ω_j and k_j are the j-th wave frequency and wavevector, respectively, and $A_j(z)$ is the corresponding

envelope, i.e., the electric field of the j-th wave is $E_j(z,t) = A_j(z)e^{i(k_j z-\omega_j t)}$. We assume slowly varying wavevectors $k_j(z)$ for each of the interacting waves and define the wavevectors mismatch $\Delta k(z) = 2k_1 - k_2$. For simplicity, we take into account the medium nonuniformity in our theory only by introducing the z dependence of the wavevectors mismatch Δk, i.e., k_j in the coupling coefficients η_j are replaced by some average values $k_{j,\mathrm{avg}}$ along the medium. Next, we define dimensionless coordinate $\zeta = z/l$ and dimensionless complex amplitudes $a_j = \eta_j^{-1/2}A_j/[\eta_1^{-1/2}|A_{1,0}|]$ where $l = [(\eta_1\eta_2)^{1/2}|A_{1,0}|]^{-1}$. In our notations, the subscript "0" denotes initial condition values. Using our definitions, we transform Eqs. (1) and (2) to the dimensionless form

$$\frac{da_1}{d\zeta} = ia_1^* a_2 e^{-il\int_0^\zeta \Delta k(\zeta')d\zeta'}, \tag{3}$$

$$\frac{da_2}{d\zeta} = i\frac{1}{2}a_1^2 e^{+il\int_0^\zeta \Delta k(\zeta')d\zeta'}. \tag{4}$$

Our next step is to represent the complex amplitudes a_j by their absolute value B_j and real phase ϕ_j by applying the definitions $a_1 = B_1\exp(i\phi_1)$ and $a_2 = B_2\exp(i[\phi_2 + l\int_0^\zeta \Delta k(\zeta')d\zeta'])$. We substitute these expressions into Eqs. (3) and (4) and decompose the resulting equations into their real and imaginary parts to obtain the following set of equations:

$$\frac{dB_1}{d\zeta} = B_1B_2\sin\Phi, \tag{5}$$

$$\frac{dB_2}{d\zeta} = -\frac{1}{2}B_1^2\sin\Phi, \tag{6}$$

$$\frac{d\Phi}{d\zeta} = l\Delta k + Q\cos\Phi, \tag{7}$$

where we defined the phase mismatch $\Phi = 2\phi_1 - \phi_2$ and $Q = B_1^2B_2(4B_1^{-2} - B_2^{-2})/2$. From the two differential equations for the real amplitudes Eqs. (5) and (6), the algebraic Manley–Rowe relation can be derived (note that according to our definitions $B_{1,0} \equiv |a_{1,0}| \equiv 1$):

$$B_1^2 + 2B_2^2 = B_{1,0}^2 + 2B_{2,0}^2 = 1 + 2B_{2,0}^2. \tag{8}$$

In the following, we assume for simplicity that the wavevector mismatch is a linear function of position and define α as the nonuniformity rate coefficient by the relation $\Delta k = \alpha(z - z_*)/l^2 = \alpha(\zeta - \zeta_*)/l$, where the subscript $*$ denotes the point of perfect wavevectors matching $\Delta k = 0$. It is convenient to introduce a shifted normalized coordinate $\xi = \zeta - z_*/l = \zeta - \zeta_*$ since the wavevectors are matched at $\xi = 0$. Equations (6) and (7) can then be rewritten as

$$\frac{dB_2}{d\xi} = -\frac{1}{2}B_1^2\sin\Phi, \tag{9}$$

$$\frac{d\Phi}{d\xi} = \alpha\xi + Q\cos\Phi. \tag{10}$$

In the rest of this paper we will focus on studying the set of two differential equations (9) and (10) for the variables B_2 and Φ in which the amplitude B_1 is expressed by Eq. (8). In Figs. 1 and 2, we present the numerical solution of Eqs. (9) and (10) as a function of the normalized distance along propagation $|\alpha|\xi$ when solving them in the interval $-20 < |\alpha|\xi < 20$ for the initial condition $B_{1,0}^2 = 1$, $B_{2,0}^2 = 0$ and $\Phi_0 = 0$. In Fig. 1 (where $\alpha = 0.1$), we see that when starting far from the wavevector matching point $|\alpha|\xi = 0$, phase-locking ($\Phi \approx \pi$) is obtained immediately. This continuous phase-locking results in a monotonic pump depletion (in average) until $|\alpha|\xi \to \sqrt{2}$ where the pump is almost completely depleted and phase-locking is lost. In Fig. 2 where the nonuniformity parameter is large ($\alpha = 10$), we see that the initial dynamics is essentially the same as in Fig. 1 but now phase-locking is maintained only until $|\alpha|\xi \approx -5$, and consequently the final conversion efficiency is much lower than in the previous example.

In the following sections we will develop an analytical theory that explains the findings that are seen in the numerical examples of Figs. 1 and 2.

3. AUTORESONANT DYNAMICS

We start the analysis at a negative value of $|\alpha|\xi_{\mathrm{ini}}$ far from the wavevector matching point, where we assume that the initial amplitude of the second harmonic wave is small, i.e. $B_{2,0} \ll B_{1,0} \equiv 1$. At first we focus on the initial stage defined by the requirement that $B_2(z) \ll B_1$. Consequently, at this stage we neglect the depletion of the pump wave and analyze only the evolution of B_2. Under these assumptions, Eqs. (9) and (10) can be approximated by

$$\frac{dB_2}{d\xi} = -\frac{1}{2}\sin\Phi, \tag{11}$$

$$\frac{d\Phi}{d\xi} = \alpha\xi - \frac{1}{2B_2}\cos\Phi, \tag{12}$$

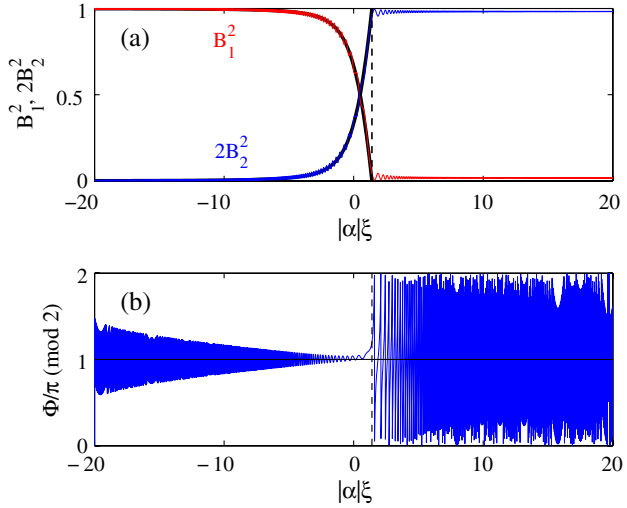

Fig. 1. Autoresonant evolution of (a) the wave envelopes B_j^2 and (b) the phase mismatch Φ versus the normalized distance $|\alpha|\xi$ for a spatial nonuniformity rate $\alpha = 0.1$. The numerical solution of Eqs. (9) and (10) is plotted by colored curves. In (a), the fundamental wave B_1 and the second harmonic wave B_2 are plotted by red and blue, respectively, and the black curves represent the value of the analytical expressions Eqs. (19) and (20). The vertical dashed line is located at $|\alpha|\xi = \sqrt{2}$ where complete pump depletion is obtained and phase-locking is lost. Note that there is an excellent agreement between the numerical solution and the analytical autoresonant solution, and the corresponding curves are overlapping until $|\alpha|\xi = \sqrt{2}$.

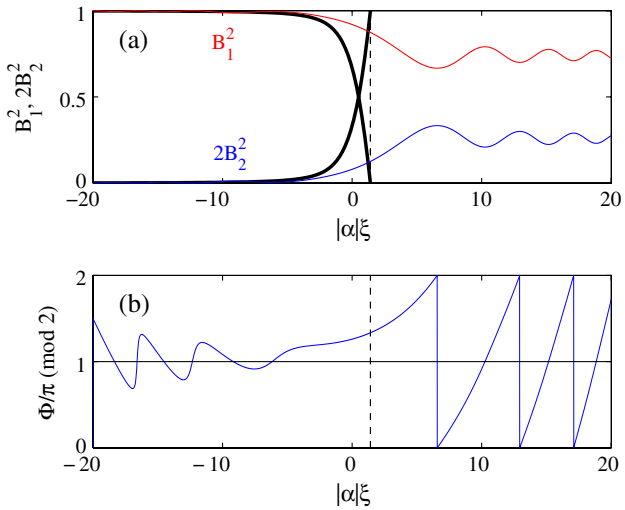

Fig. 2. Evolution of (a) wave envelopes B_j^2 and (b) phase mismatch Φ for large value of the nonuniformity rate $\alpha = 10$. Also in this case, there is a very good agreement between the numerical solution (colored lines) and the analytical autoresonant solution (black line). Note that the corresponding curves are overlapping until $|\alpha|\xi \approx -5$, where phase-locking is lost. Because of the large value of $|\alpha|$, the stability condition for autoresonance, given by Eq. (24), is not satisfied after $|\alpha|\xi \approx -5$ and consequently the final conversion efficiency is relatively low.

where we used the approximate expression $Q \approx -B_{1,0}^2/(2B_2) \equiv -1/(2B_2)$ (according to our definition of variables $B_{1,0} \equiv 1$). Note that Eqs. (11) and (12) are a particular case of Eq. (11) in [15]. Following the analysis there, we see that the solution of Eqs. (11) and (12) can be expressed in the form

$$Z = -\frac{1}{2\alpha\xi_{\text{ini}}}\left[e^{i\alpha(\xi^2-\xi_{\text{ini}}^2)/2} - \frac{\xi_{\text{ini}}}{\xi}\right], \tag{13}$$

written in terms of a single complex new variable $Z = B_2 \exp(i\Phi)$. As $|\xi|$ decreases, the term ξ_{ini}/ξ becomes dominant and Z approaches $1/(2\alpha\xi)$. Therefore, at some point our system phase-locks at $\Phi = \hat{\Phi}$ with either $\hat{\Phi} \approx \pi$ or $\hat{\Phi} \approx 0$ for α positive or negative, respectively (note that the values of $\hat{\Phi}$ are opposite to those in [15]). One can see this adiabatic initial phase-locking transition in the numerical examples in Figs. 1 and 2. At the same time B_2 grows as $B_2 = |Z| \approx 1/|2\alpha\xi|$ and thus, at some point, as $|\alpha|\xi \to -1/2$, one must also include the depletion of the fundamental wave.

We continue our analysis by taking into consideration the effect of pump depletion and assuming that the phase Φ is locked around the value $\hat{\Phi}$ [satisfying the relation $\cos\hat{\Phi} \approx -s$ where $s \equiv \text{sign}(\alpha)$]. The set of equations that describe the autoresonant phase-locked state (denoted by the hat symbol) is obtained by the requirement that the left hand side of Eq. (10) vanishes,

$$\alpha\xi - s\hat{Q} = 0, \qquad \text{i.e. } \hat{Q} = |\alpha|\xi, \tag{14}$$

and by rearranging Eq. (9):

$$\sin\hat{\Phi} = -\frac{2}{\hat{B}_1^2}\frac{d\hat{B}_2}{d\xi}. \tag{15}$$

Here $\hat{Q} = \hat{B}_1^2\hat{B}_2(4\hat{B}_1^{-2} - \hat{B}_2^{-2})/2$ can be expressed in terms of $\hat{B}_1^2$ using the Manley–Rowe relation that is given by Eq. (8). Assuming that the initial amplitude of the second harmonic wave is negligible with respect to the initial pump amplitude ($B_{2,0} \ll B_{1,0} \equiv 1$), the Manley–Rowe relation can be approximated by

$$B_1^2 + 2B_2^2 = 1. \tag{16}$$

Eliminating B_2 from Eq. (16) and substituting it in $\hat{Q}$ yields

$$\hat{Q} = \frac{2 - 3\hat{B}_1^2}{\sqrt{2(1-\hat{B}_1^2)}}. \tag{17}$$

Substituting this expression in Eq. (14) results in an algebraic equation for $\hat{B}_1$:

$$\frac{2 - 3\hat{B}_1^2}{\sqrt{2(1-\hat{B}_1^2)}} = |\alpha|\xi. \tag{18}$$

After some algebraic transformations, a quadratic equation in $\hat{B}_1^2$ can be derived from Eq. (18). The solution of our system is the root for which $\hat{B}_1^2 \to 1$ as $|\alpha|\xi \to -\infty$ that is a monotonic decreasing function of $|\alpha|\xi$, i.e.,

$$\hat{B}_1^2 = \frac{6 - (|\alpha|\xi)^2 - |\alpha|\xi\sqrt{6 + (|\alpha|\xi)^2}}{9}, \qquad |\alpha|\xi\sqrt{2}. \tag{19}$$

The solution for the second harmonic wave is obtained by substituting Eq. (19) into Eq. (16), resulting in a monotonic increasing function of $|\alpha|\xi$:

$$\hat{B}_2^2 = \frac{3 + (|\alpha|\xi)^2 + |\alpha|\xi\sqrt{6 + (|\alpha|\xi)^2}}{18}, \qquad |\alpha|\xi\sqrt{2}. \tag{20}$$

Note that our autoresonant solution predicts that if phase-locking continues, the pump could be completely depleted and all its energy will be transferred to the second harmonic wave while approaching $|\alpha|\xi = \sqrt{2}$. Beyond this point, the analytical solution that was derived becomes invalid (since $\hat{B}_1^2$ must be nonnegative), meaning that phase-locking cannot be preserved any more. The analytical solutions, Eqs. (19) and (20), are plotted in Figs. 1 and 2 and are found to be in excellent agreement with the local average of the numerical solution as long as phase-locking is preserved. In the following section, we will analyze the stability of the autoresonant state and will derive a necessary criterion for its stability, from which we could estimate what are the boundaries of the autoresonant region.

4. STABILITY OF THE PHASE-LOCKED SOLUTION

In the previous section we have discussed the autoresonant state solution that exists in our system. We show now that the phase-locked evolution of the system is stable as long as the nonuniformity rate $|\alpha|$ is small enough. In studying the stability, we assume that the solution is close to the autoresonant state, i.e., we consider $B_2 = \hat{B}_2 + \delta B_2$ and $\Phi = \hat{\Phi} + \delta\Phi$ where $|\delta B_2|$, $|\delta\Phi| \ll 1$. In our analysis we apply the approximate trigonometric relations $\sin\Phi = -s\sin\delta\Phi$ and $\cos\Phi \approx -s$ (derived from $\sin\hat{\Phi} = 0$ and $\cos\delta\Phi \approx 1$). We start by replacing $\cos\Phi$ by $-s$ in Eq. (10) and expanding the equation to first order in δB_2:

$$\frac{d\Phi}{d\xi} = s(|\alpha|\xi - \hat{Q}) - s\hat{Q}'\delta B_2, \tag{21}$$

where $\hat{Q}'$ denotes the derivation of Q with respect to B_2 evaluated at $\hat{B}_2$. Recalling that phase-locking ($d\hat{\Phi}/d\xi = 0$) is defined by Eq. (14), we see that

$$\frac{d(\delta\Phi)}{d\xi} = -s\hat{Q}'\delta B_2. \tag{22}$$

The following differential equation for δB_2 is obtained by substituting the relation $d\hat{B}_2/d\xi = |\alpha|/\hat{Q}'$ [derived by differentiation of Eq. (14)] and the lowest order expansion of Eq. (9) in the variables δB_2, $\delta\Phi$, into the relation $d(\delta B_2)/d\xi = dB_2/d\xi - d\hat{B}_2/d\xi$:

$$\frac{d(\delta B_2)}{d\xi} = s\frac{\hat{B}_1^2}{2}\sin\delta\Phi - \frac{|\alpha|}{\hat{Q}'}, \tag{23}$$

where we used $\sin\Phi = -s\sin\delta\Phi$. Equations (22) and (23) are the Hamilton equations for the canonical variables δB_2 and $\delta\Phi$ that are related to the Hamiltonian

$$H(\delta B_2, \delta\Phi, \xi) = -s\frac{\hat{Q}'}{2}(\delta B_2)^2 + V_{\text{eff}}(\delta\Phi, \xi),$$

where $V_{\text{eff}} = s\hat{B}_1^2/2\cos\delta\Phi + |\alpha|\delta\Phi/\hat{Q}'$ and ξ acts as "time" variable. Note that V_{eff} is a tilted "washboard" potential with slow "time"-dependent parameters $\hat{B}_1$ and $\hat{Q}'$. Hence, the phase-locked state remains stable as long as the effective potential has well defined minima (since $\cos\delta\Phi \approx 1 - (\delta\Phi)^2/2$), i.e., for

$$|\alpha| < \Omega^2, \tag{24}$$

where $\Omega^2 \equiv \hat{Q}'\hat{B}_1^2/2$. An explicit expression for the spatially dependent frequency Ω is obtained by substituting Eqs. (19) and (20) into the definition of Ω^2:

$$\Omega^2 = \frac{(|\alpha|\xi)^2}{3} - \frac{2|\alpha|\xi\sqrt{(|\alpha|\xi)^2 + 6}}{3} + 2, \qquad |\alpha|\xi < \sqrt{2}. \tag{25}$$

We present the dependence of Ω^2 on $|\alpha|\xi$ in Fig. 3, where we see that Ω^2 decreases monotonically with $|\alpha|\xi$ until it vanishes at $|\alpha|\xi = \sqrt{2}$. This conclusion agrees with the finding that the spatial frequency of the small amplitude modulations that are seen in Figs. 1 and 2 around the slowly evolving average wave amplitudes [given by Eqs. (19) and (20)] and around $\hat{\Phi} \approx \pi$, decreases with $|\alpha|\xi$ (in particular, these modulations are seen well in the graphs of Φ).

In light of Eq. (24), Fig. 3 shows that for any given value of $|\alpha|$, the autoresonant state is initially stable when starting in a negative value of $|\alpha|\xi$ far from the perfect wavevector matching point $|\alpha|\xi = 0$, but it becomes unstable at some point before $|\alpha|\xi = \sqrt{2}$. Because of the decreasing dependence of Ω^2 as a function of $|\alpha|\xi$, we see that for a smaller value of $|\alpha|$, the violation of the stability criterion occurs later. Therefore, for a small enough value of the nonuniformity rate, say $|\alpha| \le 0.1$, it is possible to preserve phase-locking almost until $|\alpha|\xi = \sqrt{2}$ and practically achieve complete pump depletion. This important conclusion agrees well with the numerical results that are

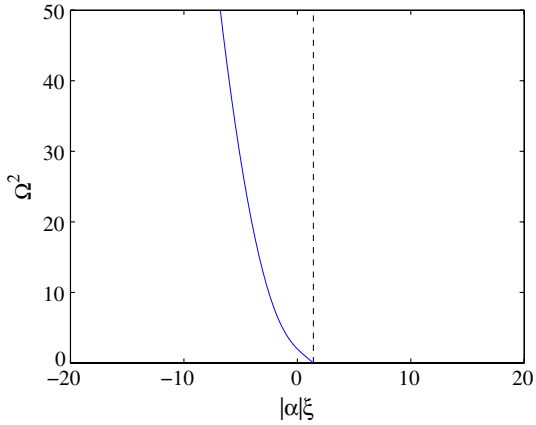

Fig. 3. Stability function Ω^2 versus $|\alpha|\xi$ given by the analytical expression in Eq. (25). Satisfying the criterion $|\alpha| < \Omega^2$ continuously is required for the stability of phase-locking.

presented in Fig. 1 for $\alpha = 0.1$. For the larger value of $\alpha = 10$ that is presented in Fig. 2, we see that phase-locking is lost at $|\alpha|\xi \approx -5$ where the stability criterion is not satisfied and the final conversion efficiency converges to about 25%, which is considerably lower when compared with the first example.

Note that even in the case of large $|\alpha|$ there are some advantages with respect to the known result in a uniform medium and arbitrary constant wavevector mismatch Δk. In the uniform case, the conversion efficiency is a periodic function of position and the spatial average conversion efficiency decreases strongly as a function of the wavevector mismatch [3]. The amplitude of the spatial oscillation is equal to the local average; hence, for any given length of a uniform medium, there are frequencies for which the final conversion efficiency is zero or close to it. Moreover, an involved dynamics occurs when relaxing the plane, monochromatic wave condition (see, e.g., [24]). On the contrary, in a nonuniform medium, the conversion efficiency increases monotonically as a function of position and could be designed to be very high within a large bandwidth. The robustness of autoresonant schemes is expected to allow achieving high conversion also in multidimensional configurations, as demonstrated for instance in [22].

In Appendix A, we derive an explicit criterion for the stability of the phase-locked solution allowing practically complete energy conversion of the initial pump energy to the second harmonic. In terms of the physical parameters, this criterion is written as

$$\frac{|\Delta k_{\text{fin}} - \Delta k_{\text{ini}}|}{L} < \frac{0.23}{l^2}, \tag{26}$$

where L is the length of the $\chi^{(2)}$ medium, Δk_{ini} and Δk_{fin} are the wavevector mismatches at the initial and the final boundaries of the medium ($\Delta k = 2\omega_1(n_1 - n_2)/c$), and

$$l = \left[\left(\frac{c\varepsilon_0}{8\pi^2}\right)\cdot\frac{n_{1,\text{avg}}^2 n_{2,\text{avg}}\lambda_1\lambda_2}{d_{\text{eff}}^2 I_{1,0}}\right]^{1/2}. \tag{27}$$

Here n_j (the subscript "avg" denotes spatial average) and λ_j denote the material refractive index and the vacuum wavelength at frequency ω_j, $I_{1,0}$ is the initial fundamental wave intensity, ε_0 is the vacuum permittivity, and c is the speed of light in vacuum.

At this point it is worth comparing the results that were obtained through our analysis of autoresonant SHG in a nonuniform medium with other autoresonant wave-mixing processes in nonuniform media that were previously studied, namely TWM and FWM [14,15]. A common feature to all these three autoresonant processes is the improvement of the conversion efficiency as the nonuniformity rate $|\alpha|$ decreases. However, while in SHG and FWM there is a well-defined point $|\alpha|\xi$ in which complete-pump depletion can be obtained, that is followed by saturation of the energy partition between the interacting waves, in TWM there is a gradual increase of the conversion efficiency as a function of position that only asymptotically may reach 100%.

5. SUMMARY

In this paper, we have analyzed the process of autoresonant SHG in a nonuniform $\chi^{(2)}$ medium. We have shown that setting a weak nonuniformity in this system allows the establishment of a stable autoresonant state in which a conversion efficiency of 100% could be obtained. We have derived closed-form analytical expressions for the spatial solution of the wave amplitudes as a function of the longitudinal coordinate [Eqs. (19) and (20)] and found a criterion for the stability of the autoresonant state [Eq. (24)]. These simple closed-form expressions could be very useful for a practical design of SHG devices. Because of the relative insensitivity of the final conversion efficiency on the system parameters, e.g., the fundamental frequency, it is expected that by choosing the design parameters appropriately, new types of highly efficient frequency converters with large bandwidths could be fabricated with potential applications in short pulses upconversion as shown in [4–8]. An estimation for the required values of the design parameters associated with autoresonant SHG devices is provided in Appendix A.

Considering the widespread use of SHG processes in various nonlinear optics configurations and their numerous applications, the authors expect that the robust autoresonant SHG scheme that is described in this paper would be relevant to a vast variety of applications. The simple explicit criteria (derived in Appendix A) that are necessary for achieving highly efficient autoresonant SHG are a valuable tool for that purpose. We stress again that these practical design criteria differ from the corresponding criteria in a TWM process in nonuniform media (see [14]), and cannot be derived from them.

Because of the insensitivity of the autoresonant scheme to small variations of the system parameters, in realistic cases in which the pump contains a range of frequencies, it is possible to obtain high conversion efficiency of each one of the spectral components of the pump (as described by our monochromatic wave model).

It should be stressed that although we considered explicitly in this paper a case in which the wavevector mismatch between the waves is a linear function of position, the actual functional dependence of the wavevector mismatch is not significant as long as it varies monotonically along propagation.

When our manuscript was under review, we became aware that some of the final conclusions of the current paper were reported also by Porat and Arie, however, by applying a completely different analysis method [25]. We find that these two separate points of view are complementary to each other, and allow together a deeper understanding of the underlying physical basis of the fundamental process of SHG in nonuniform media.

APPENDIX A: AUTORESONANT SHG DEVICE SPECIFICATIONS

In this appendix, we derive explicit formulas specifying the properties of the nonlinear medium as well as the experimental setup conditions that are required for an efficient autoresonant SHG process. At first, we express the normalized nonuniformity rate α and the position $|\alpha|\xi$ in terms of the basic physical parameters. Substituting the definitions after Eq. (2), the normalization parameter for length takes the form

$$l = \left[\left(\frac{c\varepsilon_0}{8\pi^2}\right)\cdot\frac{n_{1,avg}n_{2,avg}n_{1,0}\lambda_1\lambda_2}{d_{eff}^2 I_{1,0}}\right]^{1/2} \approx \left[\left(\frac{c\varepsilon_0}{8\pi^2}\right)\cdot\frac{n_{1,\mathrm{avg}}^2 n_{2,\mathrm{avg}}\lambda_1\lambda_2}{d_{\mathrm{eff}}^2 I_{1,0}}\right]^{1/2}, \tag{A1}$$

where we used the relations $\omega_j/k_j = c/n_j$ and $c/\omega_j = \lambda_j/2\pi$. Here n_j and λ_j denote the material refractive index and the vacuum wavelength at frequency ω_j, $I_{1,0} = 2n_{1,0}c\varepsilon_0|A_{1,0}|^2$ is the initial fundamental wave intensity, ε_0 is the vacuum permittivity, and c is the speed of light in vacuum [1]. From the definitions after Eq. (8), we see that

$$\alpha = \frac{l^2}{L}(\Delta k_{\mathrm{fin}} - \Delta k_{\mathrm{ini}}), \tag{A2}$$

and

$$\xi = \frac{l\Delta k}{\alpha} = \frac{L}{l}\cdot\frac{\Delta k}{(\Delta k_{\mathrm{fin}} - \Delta k_{\mathrm{ini}})}, \tag{A3}$$

therefore

$$|\alpha|\xi = l\cdot\Delta k\cdot\mathrm{sign}(\Delta k_{\mathrm{fin}} - \Delta k_{\mathrm{ini}}). \tag{A4}$$

Here Δk_{ini} and Δk_{fin} are the wavevector mismatches at the initial and the final boundaries of the $\chi^{(2)}$ medium, and L is the length of the nonlinear medium.

We have shown in Section 3 that the essential region of the phase-locked evolution is located between (a) $|\alpha|\xi = -1/2$ (phase-locking is achieved automatically by approaching this point) and (b) $|\alpha|\xi = \sqrt{2}$ [where complete energy conversion between the fundamental and the second harmonic wave ($B_1^2 = 0$, $2B_2^2 = 1$) may be obtained according to Eqs. (19) and (20)]. Hence, designing the variation of the parameters of the system to include the region $-1/2 < |\alpha|\xi < \sqrt{2}$ (i.e., $|\alpha|\xi_{\mathrm{ini}} \le -1/2$ and $|\alpha|\xi_{\mathrm{fin}} \ge \sqrt{2}$) will allow efficient energy conversion. From Eq. (A4) we see that it is necessary to design the system such that $\mathrm{sign}(\Delta k_{\mathrm{fin}}) \neq \mathrm{sign}(\Delta k_{\mathrm{ini}})$ and

$$|\Delta k_{\mathrm{ini}}| > \frac{1}{2l}; \qquad |\Delta k_{\mathrm{fin}}| > \frac{\sqrt{2}}{l}. \tag{A5}$$

We see that the requirements on the boundary values of the wavevector mismatch depend on the values of the length scale, which by itself is a function of various physical parameters in the system [see Eq. (28)]. For instance, an increase of the pump intensity $I_{1,0}$ results in a decrease of l and consequently in an enlargement of the necessary range of variation

of Δk that is required for allowing considerable pump depletion.

Note that the limit of a uniform medium, in which $\Delta k_{\mathrm{fin}} \to \Delta k_{\mathrm{ini}}$, is equivalent to $|\alpha| = 0$. In this case, $|\alpha|\xi \to$ const [see Eqs. (A2)–(A4)], i.e., the integration domain does not include the required interval for autoresonance $-1/2 < |\alpha|\xi < \sqrt{2}$. Therefore, in this limit, the autoresonant solution that is discussed in this paper is not applicable.

Stable phase-locked dynamics is preserved along the propagation in the system for $|\alpha| < \Omega^2$, i.e.,

$$\frac{|\Delta k_{\mathrm{fin}} - \Delta k_{\mathrm{ini}}|}{L} < \frac{\Omega^2}{l^2}, \tag{A6}$$

where Ω^2 is the expression that is given by Eq. (25). Note that Ω^2 is a monotonic decreasing function of $|\alpha|\xi$ that vanishes at $|\alpha|\xi = \sqrt{2}$; hence the stability criterion cannot be satisfied everywhere. However, keeping the phase-locking until $|\alpha|\xi = 5/4$ allows the conversion of about 90% of the initial pump energy to the second harmonic, since according to Eq. (20) at this point $2B_2^2 = 8/9$. The value of Ω^2 at $|\alpha|\xi = 5/4$ is $11/48 \approx 0.23$; therefore replacing Ω^2 in Eq. (A6) by this value gives a criterion for practically complete energy conversion.

Substituting the relation $\Delta k(z) \equiv 2k_1 - k_2 = (2n_1\omega_1 - n_2\omega_2)/c = 2\omega_1(n_1 - n_2)/c$ into Eqs. (A5) and (A6) results in an explicit criterion for efficient autoresonant conversion in terms of the properties of the medium (refractive index $n(\lambda, z)$, effective nonlinear susceptibility d_{eff} and length L) and the incident electromagnetic field (wavelength λ_1 and intensity $I_{1,0}$).

There are several possibilities to design the process of SHG in a nonuniform medium to include the point of perfect wavevectors matching ($\Delta k = 0$). One option is to use birefringent crystals in which the dispersion properties depend on the polarization of the propagating wave. Under certain conditions, it is possible to excite a second harmonic wave whose polarization is different from the polarization of the fundamental wave in such a way that a perfect wavevectors matching point will be found along their propagation direction. Another option is to design the SHG process to take place in a waveguide configuration to involve the interaction between fundamental and second harmonic waves whose modes are different from each other. Consequently, the wavevector mismatch that appears in our model has to be replaced by the mismatch between the spatially dependent propagation factors that could be designed to vanish at some point along the propagation.

ACKNOWLEDGMENTS

This work was supported by the FQRNT (Le Fonds Québécois de la Recherche sur la Nature et les Technologies) and by the NSERC (Natural Sciences and Engineering Research Council of Canada). O. Y. and L. C. wish to acknowledge the FQRNT MELS fellowship program (Files 168900 and 168739, respectively). M. C. acknowledges the support of the IOF People Programme (Marie Curie Actions) of the European Union's FP7-2012, KOHERENT, GA 299522.

REFERENCES

1. R. B. Boyd, *Nonlinear Optics*, 3rd ed. (Academic, 2008), pp. 96–104.
2. P. A. Franken, A. E. Hill, C. W. Peters, and G. Weinreich, "Generation of optical harmonics," Phys. Rev. Lett. **7**, 118–119 (1961).
3. J. A. Armstrong, N. Bloembergen, J. Ducuing, and P. S. Pershan, "Interactions between light waves in a nonlinear dielectric," Phys. Rev. **127**, 1918–1939 (1962).
4. T. Suhara and H. Nishihara, "Theoretical analysis of waveguide second-harmonic generation phase matched with uniform and chirped gratings," IEEE J. Quantum Electron. **26**, 1265–1276 (1990).
5. K. Mizuuchi, K. Yamamoto, M. Kato, and H. Sato, "Broadening of the phase-matching bandwidth in quasi-phase-matched second-harmonic generation," IEEE J. Quantum Electron. **30**, 1596–1604 (1994).
6. R. A. Haas, "Influence of a constant temperature gradient on the spectral-bandwidth of second-harmonic generation in nonlinear crystals," Opt. Commun. **113**, 523–529 (1995).
7. S. Richard, "Second-harmonic generation in tapered optical fibers," J. Opt. Soc. Am. B **27**, 1504–1512 (2010).
8. K. Regelskis, J. Žius, N. Gavrilin, and G. Račiukaitis, "Efficient second-harmonic generation of a broadband radiation by control of the temperature distribution along a nonlinear crystal," Opt. Express **20**, 28544–28556 (2012).
9. S. Longhi, "Third-harmonic generation in quasi-phase-matched $\chi^{(2)}$ media with missing second harmonic," Opt. Lett. **32**, 1791–1793 (2007).
10. M. Charbonneau-Lefort, B. Afeyan, and M. M. Fejer, "Competing collinear and noncollinear interactions in chirped quasi-phase-matched optical parametric amplifiers," J. Opt. Soc. Am. B **25**, 1402–1413 (2008).
11. H. Suchowski, D. Oron, A. Arie, and Y. Silberberg, "Geometrical representation of sum frequency generation and adiabatic frequency conversion," Phys. Rev. A **78**, 063821 (2008).
12. H. Suchowski, V. Prabhudesai, D. Oron, A. Arie, and Y. Silberberg, "Robust adiabatic sum frequency conversion," Opt. Express **17**, 12731–12740 (2009).
13. C. R. Phillips and M. M. Fejer, "Efficiency and phase of optical parametric amplification in chirped quasi-phase-matched gratings," Opt. Lett. **35**, 3093–3095 (2010).
14. O. Yaakobi, L. Caspani, M. Clerici, F. Vidal, and R. Morandotti, "Complete energy conversion by autoresonant three-wave mixing in nonuniform media," Opt. Express **21**, 1623–1632 (2013).
15. O. Yaakobi and L. Friedland, "Autoresonant four-wave mixing in optical fibers," Phys. Rev. A **82**, 023820 (2010).
16. A. Barak, Y. Lamhot, L. Friedland, and M. Segev, "Autoresonant dynamics of optical guided waves," Phys. Rev. Lett. **103**, 123901 (2009).
17. S. Trendafilov, V. Khudik, M. Tokman, and G. Shvets, "Hamiltonian description of non-reciprocal light propagation in nonlinear chiral fibers," Physica B **405**, 3003–3006 (2010).
18. M. Deutsch, B. Meerson, and J. Golub, "Strong plasma wave excitation by a chirped" laser beat wave," Phys. Fluids B **3**, 1773–1780 (1991).
19. I. Y. Dodin, G. M. Fraiman, V. M. Malkin, and N. J. Fisch, "Amplification of short laser pulses by Raman backscattering in capillary plasmas," JETP **95**, 625–638 (2002).
20. R. R. Lindberg, A. E. Charman, J. S. Wurtele, and L. Friedland, "Robust autoresonant excitation in the plasma beat-wave accelerator," Phys. Rev. Lett. **93**, 055001 (2004).
21. O. Yaakobi, L. Friedland, R. R. Lindberg, A. E. Charman, G. Penn, and J. S. Wurtele, "Spatially autoresonant stimulated Raman scattering in nonuniform plasmas," Phys. Plasmas **15**, 032105 (2008).
22. O. Yaakobi and L. Friedland, "Multidimensional, autoresonant three-wave interactions," Phys. Plasmas **15**, 102104 (2008).
23. T. Chapman, S. Huller, P. E. Masson-Laborde, W. Rozmus, and D. Pesme, "Spatially autoresonant stimulated Raman scattering in inhomogeneous plasmas in the kinetic regime," Phys. Plasmas **17**, 122317 (2010).
24. G. Valiulis, V. Jukna, O. Jedrkiewicz, M. Clerici, E. Rubino, and P. DiTrapani, "Propagation dynamics and X-pulse formation in phase-mismatched second-harmonic generation," Phys. Rev. A **83**, 043834 (2011).
25. G. Porat and A. Arie, "Efficient, broadband and robust frequency conversion by fully nonlinear adiabatic three-wave mixing," J. Opt. Soc. Am. B **30**, 1342–1351 (2013).